

NUMERICAL SIMULATION OF TURBULENT FLOW THROUGH A THREE-BLADE VERTICAL AXIS WIND TURBINE

Sina Anbaei, Masoud Ziaei-Rad, Alireza Aryaei, Ebrahim Afshari
Department of Mechanical Engineering, Faculty of Engineering, University of Isfahan, Isfahan, Iran
Corresponding author: Masoud Ziaei-Rad, e-mail: m.ziaeirad@eng.ui.ac.ir

REFERENCE NO	ABSTRACT
WIND-01	Vertical axis wind turbines (VAWT) are nowadays more of interest due to their considerable advantages despite their smaller size. This paper presents 2-D simulation of a 3-blade vertical axis wind turbine with straight blades. Governing partial differential equations of turbulent air flow are discretized and solved numerically applying finite volume method on an unstructured triangular mesh. Two-equation $k-\omega$ SST turbulence model is employed for the calculation of eddy viscosity, together with blended wall function for near-wall regions. The flow hits radially on one side of straight blades without the change in its profile along them. Also, MRF method is utilized to consider the rotation of the blades among the flow. The results of simulation demonstrated that the produced torque increases with the wind speed. The torque changes slowly at low wind speeds, but it increases more considerable at higher wind speeds, so that the slope of torque-speed graph grows as the wind speed increases. Moreover, prepared pressure-position graphs determined that pressures of both sides of blades aren't the same. The obtained results of present numerical simulation are compared with available experimental data and a good agreement with less than 15 percent of discrepancy in average is observed.

Keywords:
Vertical axis wind turbine,
Turbulent flow, straight blades,
Numerical simulation

1. INTRODUCTION

The pollution caused by the consumption of limited resources of fossil fuels obliged humanity to think of energy supply from other resources over the past decades. In this context, the idea of using and storage of renewable energies in the nature has been highly considered. Wind energy is a kind of renewable energy which is not only beneficial for the reduction of contamination and supply of clean energy, but also its sources are unlimited and it can be said that their life spans human lifetime on the earth. Modern wind turbines are divided into two main categories according to horizontal or vertical rotation of their blades: horizontal axis wind turbines (HAWT) and vertical axis wind turbines (VAWT). The first type has many applications, but its main disadvantage is that it needs a column to be positioned in the wind direction. Also, it is necessary to adjust it in the orientation of wind direction, while VAWTs are independent of wind direction, which makes them possible to be utilized in

places with changing wind blowing direction, e.g. above the residential buildings. Some other advantages of VAWTs are: good operation at low wind speeds, proper functioning on large residential buildings as small-scale energy producers, high resistance in adverse weather conditions such as snow, frost, sand and dust, lower weight, lower fabrication costs and less installation cost, no creation of unsuitable conditions for the lives of birds, ability to produce more annual power than HAWTs, high resistance at high speeds of 65 m/s, and easy maintenance of equipment such as generator, gearbox and all other main components that are installed near the ground. Taking a look at the literatures, we can find many previous studies mostly on HAWTs. Promdee and Photon [1] investigated the effect of wind angle and speed on the voltage produced by a wind turbine of the Savonius type using a double-wind tunnel test. They showed that the highest produced voltage is at the angle of 30°. Fathabadi [2] studied the maximum mechanical power obtained from a

wind turbine. He presented a new, single precision sensor, which works based on the maximum power point tracking technique. Using this sensor, he obtained the peak efficiency of 98.94%, higher than the rest of methods, with convergence time of 18 milliseconds, the shortest time of convergence among all existing methods and controllers. Kortabarria et al. [3] presented an adaptive intelligent new algorithm based on disturbance and observation method, for tracking the maximum power point in a small wind turbine. They claimed that their algorithm increases the efficiency for different wind conditions and laboratory evidence confirms their results. Kot et al. [4] compared three major algorithms for tracing and accessing the maximum power peak for a small wind turbine. Two of them work on the basis of turbine static parameters, and the other one is a series of recursive searches to find the optimal operating point. The results obtained that the third algorithm is definitely more promising, less cost and more flexible. Daili et al. [5] examined the issue of tracking and accessing the maximum power of a small wind turbine. They used a new algorithm with no mechanical sensor and showed that the proposed algorithm with dynamic responsiveness works better than conventional observation and disruption algorithm. Wang et al. [6] investigated the aerosol effects in a large wind turbine considering fluid-solid interaction. They calculated aerodynamic loads using a computational fluid dynamics model, while used finite element to analyze the static structure modules. They performed the calculations for a 1.5MW wind turbine under five different operating conditions and achieved maximum tension and compression stresses, tip deviations, and minimum structure and raw materials for each case. The effect of number of blades on the operation of a Savonius wind turbine was studied experimentally by Wenehenubun et al. [7]. They compared the wind turbines with two, three and four blades, and observed that a three-blade wind turbine has the maximum value of tip speed ratio: 0.555 was measured for the wind speed of 7 m/s. Li et al. [8]

examined the effect of turbine blades on its optimal performance employing a wind tunnel. Their results indicated that as the number of blades of vertical wind turbine increases, the power factor decreases. However, the wind power absorbed by the turbine depends on azimuth angle of upstream flow. Shen et al. [9] designed and optimized the geometry of wind turbine blades. They used finite element and lifting surface methods and explained that three-dimensional design is more efficient than two-dimensional one and that it is possible to increase the annual energy production of turbines by its 3D design. Pourrajabian et al. [10] studied the design and optimization of wind turbine blades using the theory of blade-element momentum, simple beam theory and genetic algorithm. They found that reduction in inertia of hollow blades prompts the start of movement at low velocities, as long as the stress along the blades does not exceed an allowable tension. Lin et al. [11] numerically examined the performance of a vertical-axis wind turbine with change in its rear edge. They compared tubular blades with flat blades and showed that by increasing the power and wavelength, the maximum force and the pressure coefficient grow 2.31% and 16.4%, respectively. Wang et al. [12] investigated the aerodynamic performance of blades of an inflatable turbine with adaptive blades. They changed the geometry of the blades to achieve a desired state and showed that for three different geometries, the power factor is increased by 14.56% (at low strengths) compared to a typical turbine with the same strength. They also claimed that at high strengths with low velocity ratios, the power factor is increased by 7.51% for two of their designed geometries and 8.07% for four other designations. Mescheryakov et al. [13] studied aerodynamics of a thin blade of a wind turbine, assuming high angular velocity and classical potential method; which led to a dual boundary integral equation on the surface of the blade. They found that the solution converged rapidly in two or three stages. They also tested the method on a small wind turbine and compared their results with the results of

finite element method in Fluent and CFX softwares and concluded that their method has higher speed of calculations. Li et al. [14] investigated the effect of blade strength on the aerodynamic force applied on the blade (straight blade of a vertical-axis wind turbine) using experimental measurement in a wind tunnel. They observed that by increasing the blade strength, the pressure difference between two sides of the blade decreases. Sun et al. [15] studied the optimization of a wind turbine through its aerodynamic calculations applying improved blade element momentum theory. They found that the extended theory provides better predictions in compared to its classical form.

In this paper, we numerically simulate a three-blade vertical-axis wind turbine. Two-dimensional modeling of wind turbines considering turbulent flow of the wind has not been previously studied in the literatures. Here we choose k- ω SST model for turbulence calculations which obtained reasonable results in comparison with available experimental data.

2. GEOMETRY AND ASSUMPTIONS

Figure 1 shows the geometry of a vertical axis wind turbine and rotor hub. The configuration is in a way that can shift the horizontal flow vertically to the blades.

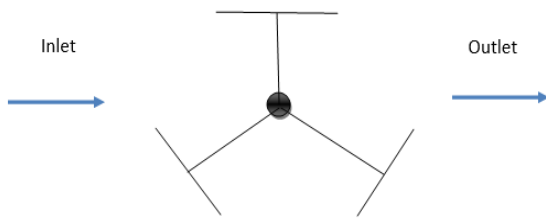


Fig.1. A schematic of studied geometry with flow direction

The air flow is supposed to be viscous, incompressible, with constant properties, uniform inflow velocity, and constant pressure at the outflow. Flow enters from the side of a two-dimensional rectangular region (which is considered as computational domain) and leaves it facing outwards. The other two sides

of the domain are solid walls. The blades are at the middle of this region.

3. MATHEMATICAL FORMULATION

The set of governing 2-D Navier-Stokes equations can be expressed in dimensional form as follow:

$$\frac{\partial u}{\partial x} + \frac{\partial v}{\partial y} = 0 \quad (1)$$

$$u \frac{\partial u}{\partial x} + v \frac{\partial u}{\partial y} = -\frac{1}{\rho} \frac{\partial p}{\partial x} + \nu_T \left(\frac{\partial^2 u}{\partial x^2} + \frac{\partial^2 u}{\partial y^2} \right) \quad (2)$$

$$u \frac{\partial v}{\partial x} + v \frac{\partial v}{\partial y} = -\frac{1}{\rho} \frac{\partial p}{\partial y} + \nu_T \left(\frac{\partial^2 v}{\partial x^2} + \frac{\partial^2 v}{\partial y^2} \right) \quad (3)$$

where x , y and z are coordinate axes, u , v and w are velocity components in x , y and z directions, respectively, p is pressure, ρ is density, and ν_T is turbulent kinematic viscosity. k- ω SST turbulence model is used in this study for calculation of turbulent viscosity. This model is a two-equation turbulence model, which employs k- ω model near the walls, while it uses k- ϵ model for free stream far from the walls. For near wall regions, the turbulence quantities are estimated by 'blended wall function'. The model is the best choice for turbulent air flow through the turbine blades, since its sensitivity to the main stream fluctuations and external aberrations is much lower than common turbulence models. Also, it is more accurate and reliable in prediction of flows with reverse pressure gradients [16].

In k- ω SST model, the transport equation for turbulent kinetic energy is written as:

$$\frac{\partial k}{\partial t} + U_j \frac{\partial k}{\partial x_j} = P_k + \beta^* k \omega + \frac{\partial}{\partial x_j} \left[(\nu + \sigma_k \nu_T) \frac{\partial k}{\partial x_j} \right] \quad (4)$$

with $\sigma_k = 0.85$ and:

$$P_k = \min \left(\tau_{ij} \frac{\partial U}{\partial x_j}, 10 \beta^* k \omega \right) \quad (5)$$

Here, k is kinetic energy of turbulent flow, ω is turbulence frequency of the flow, and ν is fluid kinematic viscosity. Also, τ is stress tensor and U is mean flow velocity. The flow frequency transport equation is expressed as follows.

$$\begin{aligned} \frac{\partial \omega}{\partial t} + U_j \frac{\partial \omega}{\partial x_j} = & a_2 S^2 - \beta \omega^2 + \\ & \frac{\partial}{\partial x_j} \left[(v + \sigma_\omega v_T) \frac{\partial \omega}{\partial x_j} \right] + \\ & 2(1 - F_1) \sigma_\omega \frac{1}{\omega} \frac{\partial k}{\partial x_j} \frac{\partial \omega}{\partial x_j} \end{aligned} \quad (6)$$

In above equation, $\alpha_2 = 0.44$, $\sigma_\omega = 0.856$, and F_1 is defined as:

$$F_1 = \tanh(R^4) \quad (7)$$

with:

$$\begin{aligned} R = \min \left[\max \left(\frac{\sqrt{k}}{\beta^* \omega y}, \frac{500v}{y^2 \omega} \right), \frac{4\sigma_\omega k}{CD_{k\omega} y^2} \right] \\ CD_{k\omega} = \max \left(2\rho\sigma_\omega \frac{1}{\omega} \frac{\partial k}{\partial x_j} \frac{\partial \omega}{\partial x_j}, 10^{-10} \right) \end{aligned} \quad (8)$$

Also, S is the average rate of strain and y is the distance measured from the wall.

Finally, the kinematic viscosity of turbulent flow can be obtained as:

$$v_T = \frac{a_1 k}{\max(a_1 \omega, SF_2)} \quad (9)$$

in which, $\alpha_1 = 5/9$, $\beta^* = 0.09$, and $F_2 = \tanh \left[\left[\max \left(\frac{2\sqrt{k}}{\beta^* \omega y}, \frac{500v}{y^2 \omega} \right) \right]^2 \right]$.

The aforementioned governing equations with appropriate boundary conditions can now be solved to obtain the flow field around the turbine blades. At inflow boundary, a certain wind speed of 38.7 m/s is considered normal to the boundary of computational domain. Moreover, turbulence intensity and viscosity ratio are set to be 5% and 10, respectively. For the flow on the surfaces of the blades, no slip boundary condition is applied.

4. NUMERICAL SCHEME

Numerical solution procedure is performed using Ansys-Fluent software (Version 18.2). It works based on finite volume method. Well-known SIMPLE algorithm computes the pressure-velocity coupling of the flow field. The method has a moderate convergence in which appropriate initial conditions push the convergence process.

The blades of studied turbine have NACA0012 profile and are made of aluminum. The blades are of straight type, and the wind flows in radial direction, causing a rotating motion.

Figure 2 shows the computational grid with triangular cells generated around the blades with fine and coarse regions. The circular region with finer grids around each blade introduces the rotating environment. The wind flow enters rectangular computational domain from the left side and leaves it from the right, where other two boundaries are taken as solid walls.

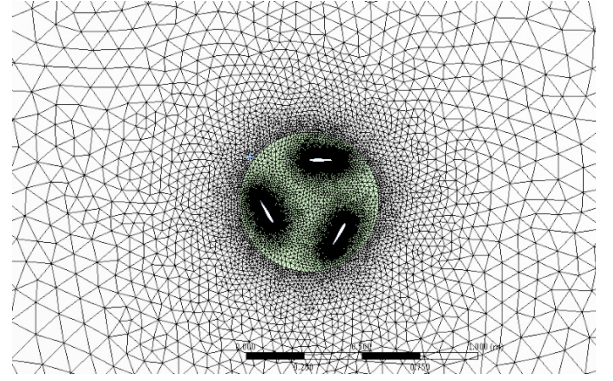


Fig.2. Applied computational grid around the blades with fine and coarse regions

In order to simulate the rotation of the blades, we use MRF ‘Multiple Rotating Reference Frame’ method. By selecting MRF, it is possible to have a steady solution. In this scheme, instead of blades rotation, they are supposed to be fixed and the flow rotates around them, i.e. we can use a fixed coordinate system. The advantage of this method is to pay less time and computational cost in comparison to a dynamic mesh with the rotation of blades.

5. RESULTS AND DISCUSSION

To ensure the quality of computational grid and the accuracy of numerical scheme, we investigate the independency of our results to the number of computational nodes. To do this, we can change the number of cells and check if it makes significant change in the results. A graph of this process is shown in fig.3. The figure indicates that as the number of elements exceeds 500,000, no significant change can be observed in output torque. Therefore, the most economical number of possible computational nodes is 500,000 at this wind speed.

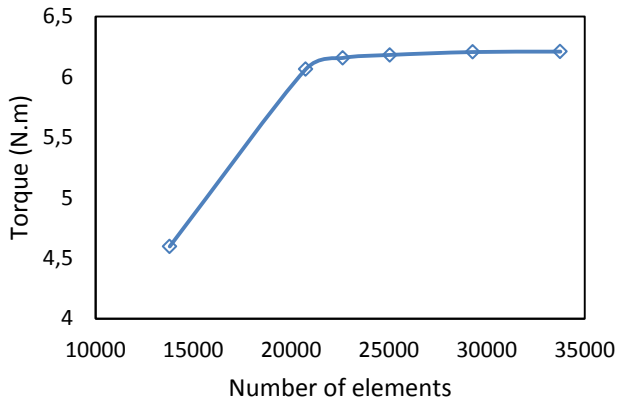


Fig.3. Independency of numerical outputs to the number of computational nodes ($U = 19.38$ m/s)

Moreover, we checked the value of y^+ near the wall to find its appropriate range for applied turbulence model. For $k-\omega$ SST model, we used ‘blended wall function’ for near-wall computations. As we can see in fig.4, the value of y^+ does not exceed 5 for two different wall sides, ensuring the accuracy of computed parameters in this region.

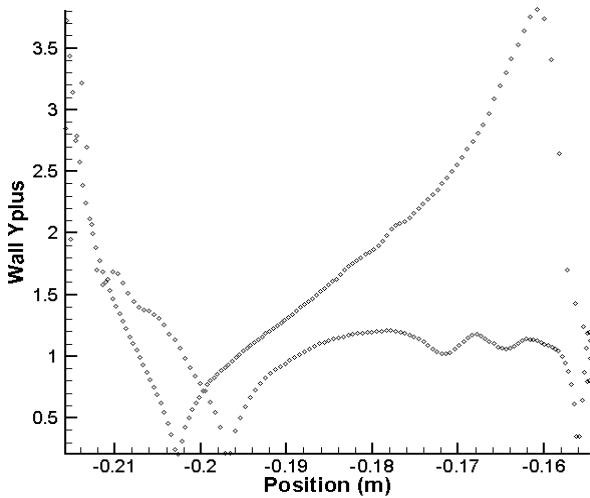
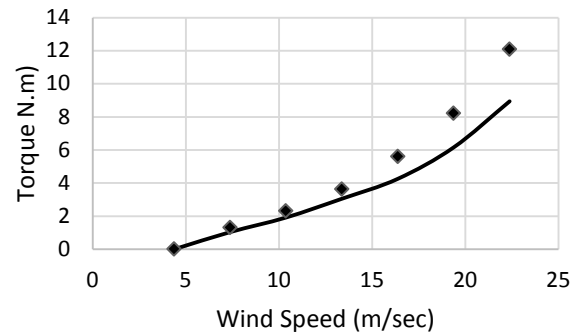


Fig.4. Appropriate range of y^+ near the wall for two different wall sides

The numerical procedure and outcome results are also verified by available experimental data in fig. 5. In this case, we compared the results of numerical simulation with data of a vertical axis wind turbine with NACA0012 blade profile, made of aluminum. The blades are of straight type and the wind blows radially in one direction, causing rotational movement (the rest of information is in Ref. [16]). The graph shows a torque value of zero before the wind speed of 5m/s. In all wind

turbines, the energy needed for the initial rotation of blades is considerable. Hence, there's no rotation before this speed. The lower slope for the graph at low speeds is also due to this fact. However, at high wind speeds, the change in the torque increases significantly. For instance, the difference in torque from 5 to 10 m/s of the wind speed is 2 N.m, while it is 4 N.m for the range of 15 to 20 m/s. A good agreement can be seen between numerical results and experimental data.



◆ Experimental — Numerical Simulation

Fig.5. comparison of torque vs. wind speed for a peripheral wind turbine with experimental measurement in wind tunnel [16]

Figures 6 and 7, respectively, plot the pressure and velocity contours around the blades obtained at the wind speed of 7.38 m/s. Significant changes in the pressure and velocity at the vicinity of the blades force them to move. The pressure difference created on both sides of a blade (red vs. blue parts) generates a propulsion force which rotates the turbine.

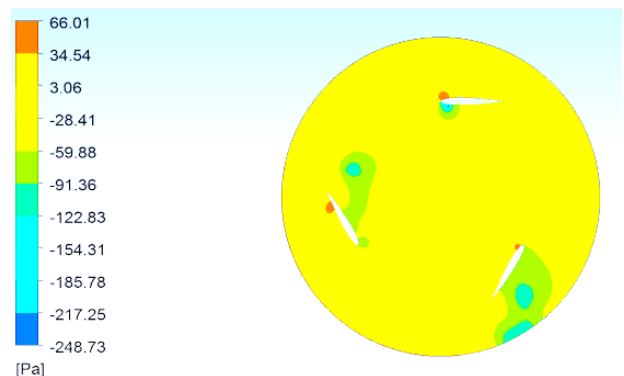


Fig.6. Pressure contour around turbine blades at the wind speed of 7.38 m/s

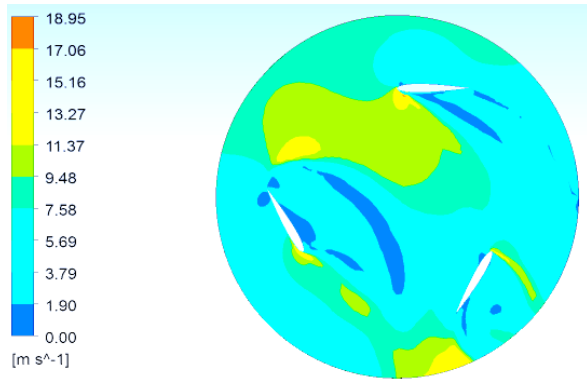
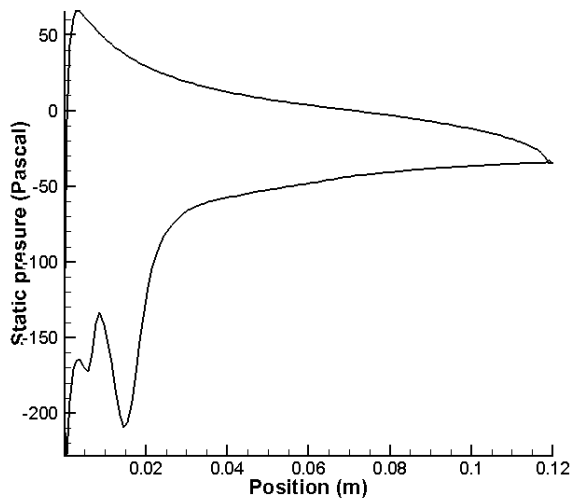
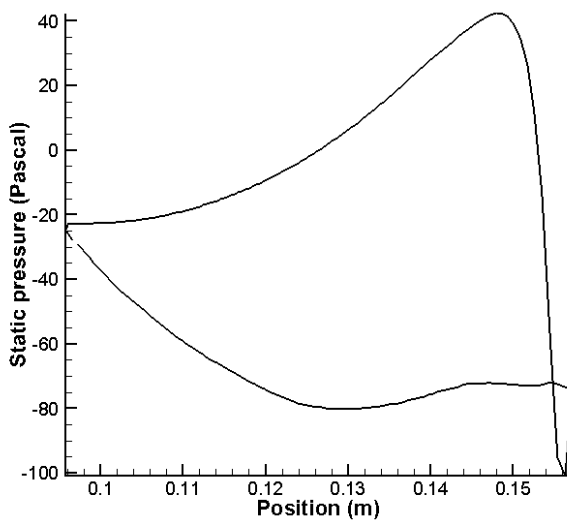


Fig.7. Velocity contour around turbine blades at the wind speed of 7.38 m/s

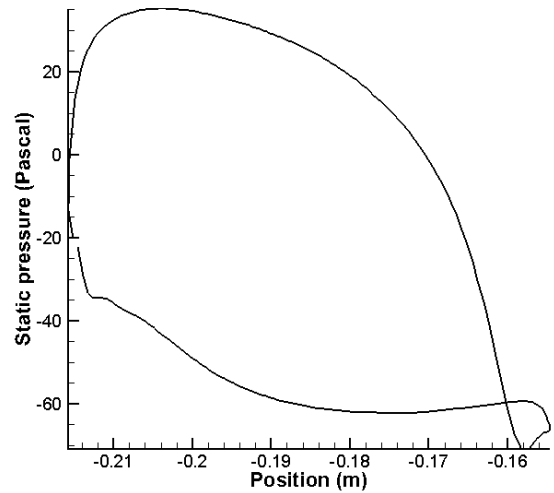
The pressure at different positions of two sides on the blades is shown in fig. 8. These plots clearly indicate that the pressure difference created on both sides of a blade causes a necessary force for its movement.



(a)



(b)



(c)

Fig.8. Pressure difference on both sides of the blades for three different positions on the blades

Since the air flows in radial direction, the pressure differences on each side of blades are different. The horizontal axis of each graph represents the path traversed on the blade, given that there are two directions on each blade, therefore, two close curves are plotted for both sides of the blade.

6. CONCLUSION

This paper presented two-dimensional simulation of turbulent flow through a 3-blade vertical axis wind turbine with straight fixed-profile aluminum blades. We used Ansys-Fluent software to simulate and analyze the environment of a wind tunnel includes turbine blades. The flow hits the blades radially. MRF method was applied to simulate the rotation of the blades. The results showed that the torque produced by this turbine enhances as the wind speed increases. The slope of this torque-speed graph first ascends slowly and then increases significantly with the wind speed. Moreover, the graphs of pressure difference on two sides of the blades represent a good sight of blades rotation. Also, obtained results indicated that present 2D simulation has a discrepancy less than 15 percent relative to available experimental data, confirming the accuracy and reliability of numerical results.

References

- [1] C. Promdee, C. Photon, effects of wind angles and wind speeds on voltage generation of Savonius wind turbine with double wind tunnels, *Procedia Computer Science*, Vol. 86, No. 6, 2016, pp. 401-404.
- [2] H. Fathabadi, Maximum mechanical power extraction from wind turbines using novel proposed high accuracy single-sensor-based maximum power point tracking technique, *Energy*, Vol. 113, No. 12, 2016, pp. 1219-1230.
- [3] I. Kortabarria, J. Andreu, J. Martínez de Alegría, J. Jiménez, J. Ignacio Gárate, E. Robles, A novel adaptive maximum power point tracking algorithm for small wind turbines, *Renewable Energy*, Vol. 63, No. 17, 2014, pp. 785-796.
- [4] R. Kot, M. Rolak, M. Malinowski, Comparison of maximum peak power tracking algorithms for a small wind turbine, *Mathematics and computers in simulation*, Vol. 91, No. 21, 2013, pp. 29-40.
- [5] Y. Daili, J. Gaubert, L. Rahmani, Implementation of a new maximum power point tracking control strategy for small wind energy conversion systems without mechanical sensors, *Energy Conversion and Management*, Vol. 97, No. 33, 2015, pp. 298-306.
- [6] L. Wang, R. Quant, A. Kolios, Fluid structure interaction modelling of horizontal-axis wind turbine blades based on CFD and FEA, *Journal of Wind Engineering and Industrial Aerodynamics*, Vol. 158, No. 2, 2016, pp. 11-25.
- [7] F. Wenehenubun, A. Saputra, H. Sutanto, An experimental study on the performance of Savonius wind turbines related with the number of blades, *Energy procedia*, Vol. 68, No. 7, 2015, pp. 297-304.
- [8] Q. Li, T. Maeda, Y. Kamada, J. Murata, K. Furukawa, M. Yamamoto, Effect of number of blades on aerodynamic forces on a straight-bladed Vertical Axis Wind Turbine, *Energy*, Vol. 90, No. 14, 2015, pp. 784-795.
- [9] X. Shen, H. Yang, J. Chen, X. Zhu, Z. Du, Aerodynamic shape optimization of non-straight small wind turbine blades, *Energy Conversion and Management*, Vol. 119, No. 16, 2016, pp. 266-278.
- [10] A. Pourrajabian, P. Nazmi Afshar, M. Ahmadizadeh, D. Wood, Aero-structural design and optimization of a small wind turbine blade, *Renewable Energy*, Vol. 87, No. 24, 2016, pp. 837-848.
- [11] S. Lin, Y. Lin, C. Bai, W. Wang, Performance analysis of vertical-axis-wind-turbine blade with modified trailing edge through computational fluid dynamics, *Renewable Energy*, Vol. 99, No. 31, 2016, pp. 654-66.
- [12] Y. Wang, X. Sun, X. Dong, B. Zhu, D. Huang, Z. Zheng, Numerical investigation on aerodynamic performance of a novel vertical axis wind turbine with adaptive blades, *Energy Conversion and Management*, Vol. 108, No. 28, 2016, pp. 275-286.
- [13] K. Mescheryakov, M. Sumbatyan, A. Bondarchuk, A boundary integral equation over the thin rotating blade of a wind turbine, *Engineering Analysis with Boundary Elements*, Vol. 71, No. 32, 2016, pp. 20-26.
- [14] Q. Li, T. Maeda, Y. Kamada, J. Murata, K. Shimizu, T. Ogasawara, A. Nakai, T. Kasuya, Effect of solidity on aerodynamic forces around straight-bladed vertical axis wind turbine by wind tunnel experiments (depending on number of blades), *Renewable Energy*, Vol. 96, No. 41, 2016, pp. 928-939.
- [15] Z. Sun, J. Chen, W. Zhong Shen, W. Jun Zhu, Improved blade element momentum theory for wind turbine aerodynamic computations, *Renewable Energy*, Vol. 96, No. 35, 2016, pp. 824-831.
- [16] K.A. Sunny, N.M. Kumar, Vertical axis wind turbine: Aerodynamic modelling and its testing in wind tunnel, *Procedia Computer Science*, Vol. 93, No. 15, 2016, pp. 1017-1023.